




# Bimodal Response to Shiga Toxin 2 Subtypes Results from Relatively Weak Binding to the Target Cell

Patrick Cherubin,<sup>a\*</sup> Dennis Fidler,<sup>a</sup>  Beatriz Quiñones,<sup>b</sup> Ken Teter<sup>a</sup>

<sup>a</sup>Burnett School of Biomedical Sciences, College of Medicine, University of Central Florida, Orlando, Florida, USA

<sup>b</sup>United States Department of Agriculture–Agricultural Research Service, Western Regional Research Center, Produce Safety and Microbiology Research Unit, Albany, California, USA

**ABSTRACT** There are two major antigenic forms of Shiga toxin (Stx), Stx1 and Stx2, which bind the same receptor and act on the same target but nonetheless differ in potency. Stx1a is more toxic to cultured cells, but Stx2 subtypes are more potent in animal models. To understand this phenomenon in cultured cells, we used a system that combines flow cytometry with a fluorescent reporter to monitor the Stx-induced inhibition of protein synthesis in single cells. We observed that Vero cells intoxicated with Stx1a behave differently than those intoxicated with Stx2 subtypes: cells challenged with Stx1a exhibited a population-wide loss of protein synthesis, while cells exposed to Stx2a or Stx2c exhibited a dose-dependent bimodal response in which one subpopulation of cells was unaffected (i.e., no loss of protein synthesis). Cells challenged with a hybrid toxin containing the catalytic subunit of Stx1a and the cell-binding subunit of Stx2a also exhibited a bimodal response to intoxication, while cells challenged with a hybrid toxin containing the catalytic subunit of Stx2a and the cell-binding subunit of Stx1a exhibited a population-wide loss of protein synthesis. Other experiments further supported a primary role for the subtype of the B subunit in the outcome of host-Stx interactions. Our collective observations indicate that the bimodal response to Stx2 subtypes is due to relatively weak binding between Stx2 and the host cell that reduces the total functional pool of Stx2 in comparison to that of Stx1a. This explains, in part, the molecular basis for the differential cellular toxicity between Stx1a and Stx2 subtypes.

**KEYWORDS** *Escherichia coli*, flow cytometry, Shiga toxin, Stx1, Stx2, Vero, Shiga toxins

Shiga toxin-producing *Escherichia coli* (STEC) strains are a major public health concern worldwide, and STEC serotype O157:H7 is associated with human gastroenteritis in industrialized countries (1–5). STEC infections can range from mild to life-threatening conditions such as hemolytic-uremic syndrome, and the production of Shiga toxin (Stx) has been associated with severe disease symptoms in humans (4, 6). Stx has a catalytic A subunit (StxA) and a pentameric receptor binding B subunit (StxB), which places it in the family of AB<sub>5</sub>-type toxins (7). StxA is proteolytically nicked to generate a disulfide-linked heterodimer composed of an enzymatic A1 fragment and an A2 fragment that extends into the central pore of the ring-like StxB homopentamer. Stx binding to globotriaosylceramide (Gb3) or globotetraosylceramide (Gb4) on the surface of a target cell leads to endocytosis through clathrin-coated pits (8–10). Furin cleaves the holotoxin-associated StxA subunit in the endosomes and/or *trans*-Golgi network to generate the StxA1/StxA2 heterodimer (11). The toxin then moves by retrograde transport to the endoplasmic reticulum (ER), where reduction of the StxA1/StxA2 disulfide bond allows StxA1 to dissociate from the rest of the toxin before entering the cytosol (12). In the cytosol, StxA1 irreversibly inactivates the ribosome through the

**Citation** Cherubin P, Fidler D, Quiñones B, Teter K. 2019. Bimodal response to Shiga toxin 2 subtypes results from relatively weak binding to the target cell. *Infect Immun* 87:e00428-19. <https://doi.org/10.1128/IAI.00428-19>.

**Editor** Shelley M. Payne, The University of Texas at Austin

**Copyright** © 2019 American Society for Microbiology. All Rights Reserved.

Address correspondence to Ken Teter, kteter@mail.ucf.edu.

\* Present address: Patrick Cherubin, Department of Pathology and Lab Medicine, The Perelman School of Medicine, The Children's Hospital of Philadelphia, University of Pennsylvania, Philadelphia, Pennsylvania, USA.

**Received** 30 May 2019

**Returned for modification** 26 June 2019

**Accepted** 7 September 2019

**Accepted manuscript posted online** 16 September 2019

**Published** 18 November 2019

depurination of an adenine residue in the 28S rRNA of the 60S ribosomal subunit. This interferes with protein translation, ultimately resulting in apoptotic cell death (13, 14).

There are two major antigenic forms of Stx, Stx1 and Stx2 (15). Both are ~70-kDa AB<sub>5</sub>-type toxins. Three subtypes of Stx1 have been classified, Stx1a, Stx1c, and Stx1d (16). Stx2, on the other hand, is composed of a diverse and heterogeneous group of subtypes, from Stx2a to Stx2h (17–19). These subtypes differ in potency and species specificity, with Stx2a, Stx2c, and Stx2d linked to severe human illness (20–24). Stx2a is associated with more severe infections than the other Stx2 subtypes or Stx1a (6, 21, 25–27). In contrast, Stx1a is more toxic to cultured Vero cells than Stx2a or Stx2c (28, 29). The factors contributing to these differences are not fully understood.

The B subunits of Stx1a and Stx2a share nearly 60% sequence similarity and use the same Gb3 globoside as their primary surface receptor (30, 31), but several studies have nonetheless highlighted the role of the B subunit in the differential toxicity of Stx subtypes (29, 32, 33). The B subunits of Stx2a and Stx2c only differ by two amino acids, but the difference at residue 16 is responsible for the higher *in vitro* affinity of Stx2a for Gb3 and the greater toxicity of Stx2a than Stx2c (34). *In vitro*, Stx1a has a greater affinity than Stx2a for Gb3 (28, 33, 35–37). A study by Russo et al. (38) has further shown that a hybrid Stx comprising the A1 subunit of Stx1a with the A2 and B subunits of Stx2a (Stx 122) is less potent in Vero cells than a hybrid toxin comprised of the A1 subunit of Stx2a with the A2 and B subunits of Stx1a (Stx 211). These collective observations have led to a model suggesting that the B subunit is responsible for the differential potency of Stx subtypes. Yet, Basu et al. (39) reported that the A1 subunit of Stx2a has a higher affinity for the ribosome and higher catalytic activity than Stx1a. Thus, the A1 subunit could also contribute to the differential potency of Stx subtypes. Further studies on the cellular actions of the A and B subunits are therefore needed in order to better understand the differential toxicity between Stx subtypes.

Here, we examined the basis for the different cellular potencies of Stx subtypes. Flow cytometry in conjunction with a green fluorescent protein (GFP) reporter system was used to monitor the Stx-induced inhibition of protein synthesis in single cells. With this strategy, we documented a dose-dependent bimodal response to Stx2 subtypes, namely, one subpopulation of cells exposed to Stx2a or Stx2c exhibited the expected loss of protein synthesis, but another subpopulation was completely resistant to intoxication and exhibited no loss of protein synthesis. In contrast, cells exposed to Stx1a exhibited a uniform, population-wide loss of protein synthesis. The bimodal response to Stx2a or Stx2c has not been previously reported, so we performed a comparative analysis between Stx1a and Stx2a to further examine this phenomenon. We found that no pool of cells was intrinsically resistant to Stx2 subtypes. All cells in the population expressed both Gb3 and Gb4, and all cells in the population could bind the B subunit from Stx2a. Additional studies documented stronger binding of Stx1a than Stx2a to target cells, with the subtype of the toxin B subunit being responsible for either the uniform or bimodal response to toxin. Collectively, these observations indicate that the bimodal response to Stx2 subtypes is due to a relatively weak binding between Stx2 and the host cell that reduces the cytosolic pool of Stx2 in comparison to that of Stx1a. This explains, in part, the molecular basis for the differential cellular toxicity between Stx1a and Stx2 subtypes.

## RESULTS

**Stx1a is more potent than Stx2 subtypes against cultured cells.** Vero-d2EGFP cells were used to establish the relative potencies of Stx1a, Stx2a, and Stx2c. These cells express a destabilized variant of enhanced green fluorescent protein (EGFP) with a 2-h half-life, so ongoing protein synthesis is required to maintain the EGFP fluorescent signal (40). Cells were seeded on a 96-well plate overnight before an 18-h incubation with 10-fold serial dilutions of each toxin. Stx1a was very effective at inhibiting protein synthesis in the target cells, with a 50% effective dose (ED<sub>50</sub>) of 0.005 ng/ml (Fig. 1A, triangles). Stx2a was less effective than Stx1a, with a 140-fold higher ED<sub>50</sub> of 0.7 ng/ml (Fig. 1A, circles). An ED<sub>50</sub> of 10 ng/ml was recorded for Stx2c (Fig. 1A, squares), which

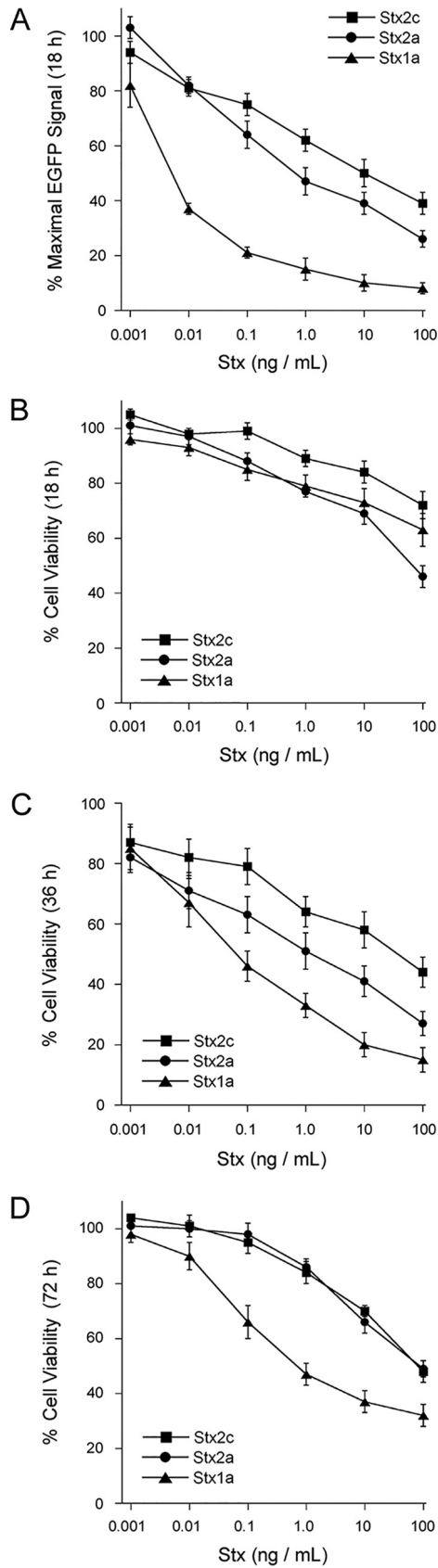


**FIG 1** Relative potencies of Stx subtypes. Vero-d2EGFP cells were challenged with 10-fold serial dilutions of Stx1a (triangles), Stx2a (circles), or Stx2c (squares). The extent of protein synthesis after 18 h of (Continued on next page)

was 2,000-fold less toxic than Stx1a. Our results were consistent with previous reports on the relative cellular activities of Stx1a, Stx2a, and Stx2c (15, 28, 29).

As previously observed when examining the toxicity of Stx1a in Vero cells (41), there was a greater level of protein synthesis inhibition than cell death after an 18-h intoxication with Stx2a and Stx2c subtypes (Fig. 1A and B). Extending the toxin challenge to 36 h resulted in greater cell death than that seen at 18 h (Fig. 1C). ED<sub>50</sub> values for cell viability after a 36-h toxin exposure demonstrated that Stx1a (ED<sub>50</sub> of 0.06 ng/ml) was 17-fold more potent than Stx2a (ED<sub>50</sub> of 1 ng/ml) and 667-fold more potent than Stx2c (ED<sub>50</sub> of 40 ng/ml). Thus, consistent with previous reports (15, 28, 29), Vero cells were much more sensitive to Stx1a than either Stx2a or Stx2c, as determined by both protein synthesis and cell viability assays. Extending the toxin challenge to 72 h did not result in greater levels of cell death than those seen after 36 h of toxin exposure (Fig. 1D). In fact, cell viability trended upward at 72 h for all toxin concentrations. This finding indicated that a substantial number of cells survived the ongoing toxin incubation and were continuing to grow.

**Bimodal cellular response to Stx2 subtypes.** With our Vero-d2EGFP system, the toxin-induced loss of protein synthesis can be detected with a plate reader or by flow cytometry. Both methods recorded the same level of toxin activity on cells incubated overnight with Stx1a (41). Previous analyses using flow cytometry further documented the population-wide loss of protein synthesis in cells exposed to Stx1a (41), which was replicated here, namely, increasing concentrations of Stx1a elicited an increasingly dramatic downshift in the peak fluorescent intensity of Vero-d2EGFP cells (Fig. 2A). This effect was not seen for cells challenged with Stx2a (Fig. 2B) or Stx2c (Fig. 2C). Both toxins generated a bimodal fluorescent profile from the intoxicated Vero-d2EGFP cells, in which one subpopulation of cells maintained the peak fluorescent intensity observed for unintoxicated cells and the other subpopulation exhibited reduced levels of fluorescent intensity (i.e., protein synthesis). A substantial number of Vero-d2EGFP cells were therefore resistant to moderate doses of Stx2a and Stx2c, with no appreciable loss of protein synthesis. The subpopulation of Vero cells that maintained the peak fluorescent intensity after challenge with Stx2a or Stx2c were not intrinsically resistant to the toxins, however, as the subpopulation of resistant cells progressively decreased with increasing toxin concentrations (Fig. 2B and C). This indicated that Stx2a and Stx2c can generate substantial, population-wide decreases in protein synthesis when present at relatively high toxin concentrations of 10 ng/ml or greater.

**Uniform distribution of Gb3 and Gb4 in the population of Vero cells.** Globoside Gb3 serves as a functional surface receptor for all Stx subtypes, including Stx2e, which preferably binds to the Gb4 surface receptor (7, 36, 37, 42–45). Gb4 also has a moderate affinity for Stx1a and a weak affinity for Stx2a or Stx2c. We accordingly predicted that the Stx2a/Stx2c-resistant subpopulation of Vero cells lacked Gb3 but still expressed the alternate Gb4 receptor with preferential affinity for Stx1a. To test this hypothesis, we examined the distribution of Gb3 and Gb4 in a population of Vero cells. Analysis by flow cytometry documented a uniform distribution of Gb3 (Fig. 3A) and Gb4 (Fig. 3B) in cell populations exposed to Gb3 or Gb4 primary antibodies and fluorophore-labeled secondary antibodies, which, in agreement with previous studies (45–47), confirmed that the population of Vero cells employed for these experiments contained both Gb3 and Gb4 cell surface receptors.

Vero cells were next incubated with both Gb3 and Gb4 antibodies and then with the corresponding fluorophore-labeled secondary antibodies. Preliminary experiments confirmed that the signals from each fluorophore did not bleed into the emission wavelength of the other fluorophore (data not shown). A scatter plot of the resulting data

**FIG 1** Legend (Continued)

incubation (A) or cell viability after 18 h (B), 36 h (C), and 72 h (D) of incubation was then recorded. Values for toxin-treated cells were expressed as percentages of the maximal signal obtained from unintoxicated control cells. Data represent the means  $\pm$  standard errors of the means of at least 6 independent experiments with 6 replicate samples per experiment.

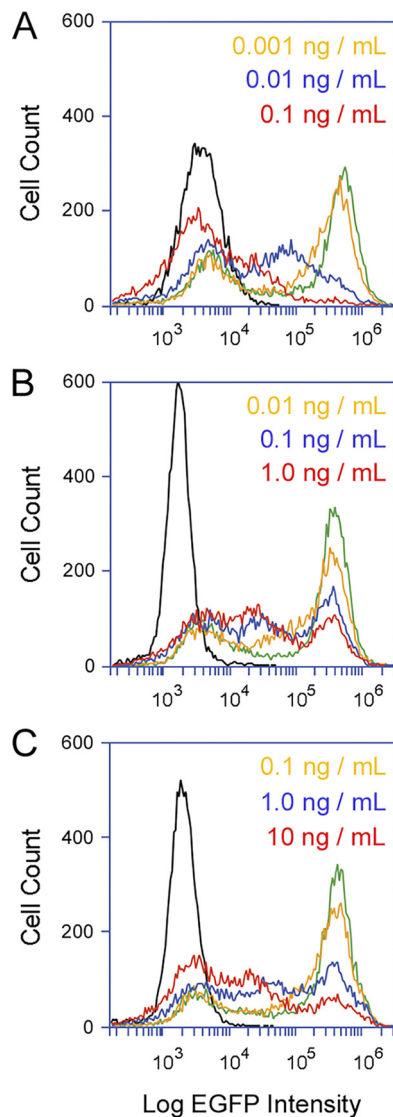


**FIG 2** Distinct cellular responses to Stx subtypes. Vero-d2EGFP cells were subjected to cytofluorometry after an 18-h incubation with the stated concentrations of Stx1a (A), Stx2a (B), or Stx2c (C). Unintoxicated parental Vero cells (black lines) and unintoxicated Vero-d2EGFP cells (green lines) were also processed for each condition. One of three representative experiments is shown.

revealed a linear relationship between the two globosides, indicating that Gb3 content was proportional to Gb4 content (Fig. 3C). Only 3% of cells were positive for Gb3 but not Gb4 (lower right quadrant), and only 5% of cells were positive for Gb4 but not Gb3 (upper left quadrant). Therefore, contrary to our hypothesis, the collective experiments with Gb3 and Gb4 staining suggested that nearly the entire population of Vero cells expresses both Gb3 and Gb4. The minor population of Gb3<sup>-</sup>/Gb4<sup>+</sup> cells (5%) could not account for the relatively high number of cells that were completely resistant to moderate concentrations of Stx2a or Stx2c (Fig. 2B and C).

**The B subunit of Stx1a binds to host cells with better efficiency than that of Stx2a.** To further examine the dose-dependent binding of the B subunits of Stx1a or Stx2a with their surface receptors, Vero cells were incubated with the fluorophore-labeled B subunits for 30 min at 4°C before analysis by flow cytometry (Fig. 4). A uniform distribution of toxin binding was observed in cells exposed to the B subunits of either Stx1a (Fig. 4A) or Stx2a (Fig. 4B). As seen for the distribution of Gb3 and Gb4 (Fig. 3), there was no obvious subpopulation of cells that did not bind the B subunit.

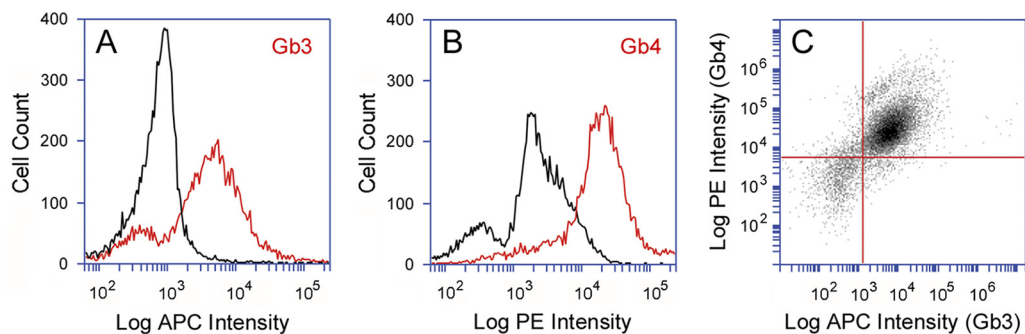


**FIG 3** Gb3 and Gb4 distribution in Vero cells. Gb3 and Gb4 antibodies were applied independently (A and B) or simultaneously (C) to Vero cells before analysis by cytofluorometry. (A) Staining pattern for the combination of a rat antibody against Gb3 and an allophycocyanin (APC)-conjugated goat anti-rat IgG antibody (red line). (B) Staining pattern for the combination of a rabbit antibody against Gb4 and a phycoerythrin (PE)-conjugated donkey anti-rabbit IgG antibody (red line). Cells incubated with the secondary antibody alone (black lines in panels A and B) were processed as well. (C) The combined staining patterns for Gb3 and Gb4 are represented on a scatter plot of 10,000 individual cells. Cells exposed to secondary antibody alone were used to set background gates represented by the red lines.

The labeling efficiency for the B subunit of Stx1a (0.093) was slightly weaker than the labeling efficiency for the B subunit of Stx2a (0.13), yet a stronger cell-binding signal was recorded for the B subunit of Stx1a than Stx2a when  $1 \mu\text{g}$  of each  $\sim 8\text{-kDa}$  B subunit was tested (Fig. 4C). Figure 4D further shows that  $0.5 \mu\text{g}$  of the Stx2a B subunit was required to generate the same cell-binding signal as  $0.2 \mu\text{g}$  of the Stx1a B subunit. Similar observations were made for other pairs of toxin concentrations (i.e., equivalent fluorescent signals from the B subunits of Stx1a and Stx2a required a greater concentration of the Stx2a B subunit; data not shown). Our observations of better cell binding for the B subunit of Stx1a than that of Stx2a were consistent with reports that have documented a higher affinity for the interaction between Stx1a and cultured mammalian cell receptors than for Stx2a (29, 33, 36).

Competition assays further emphasized the different affinities of Stx1a and Stx2a for Vero cells (Fig. 5). In this experiment, a fixed concentration of Stx1a ( $0.1 \text{ ng/ml}$ ) was mixed with one of two different concentrations of Stx2a ( $1 \text{ ng/ml}$  and  $10 \text{ ng/ml}$ ). Flow cytometry was then used to assess the effect on protein synthesis after 18 h in the presence of Stx1a, Stx2a, or both. Cells exposed to Stx1a alone (Fig. 5A) exhibited a uniform drop in protein synthesis, whereas cells exposed to either concentration of Stx2a alone exhibited a bimodal response (Fig. 5B). These results were consistent with the data presented in Fig. 2 and expanded upon those experiments by using a  $10\text{-ng/ml}$  concentration of Stx2a that, as determined by Fig. 1A, resulted in a 61%

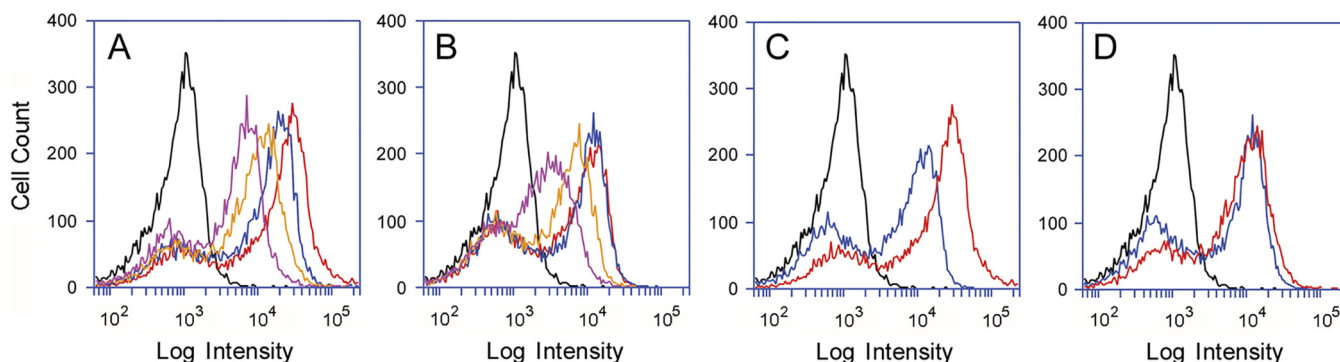


**FIG 4** Dose-dependent association of Stx1a and Stx2 with the cell surface. Vero cells were processed for cytofluorometry after a 30-min  $4^\circ\text{C}$  incubation with the fluorophore-labeled B subunits of Stx1a or Stx2a. (A and B) Cells were incubated without toxin (black line) or in the presence of various quantities of either the Stx1a B subunit (A) or Stx2a B subunit (B) at  $0.2 \mu\text{g}$  (magenta line),  $0.5 \mu\text{g}$  (yellow line),  $1.0 \mu\text{g}$  (blue line), or  $2.0 \mu\text{g}$  (red line), all in a  $500\text{-}\mu\text{l}$  volume. (C) The signals recorded for  $2 \mu\text{g}$  of either the Stx1a B subunit (red line) or Stx2a B subunit (blue line) were overlaid on the same plot. (D) The signals recorded for  $0.2 \mu\text{g}$  of the Stx1a B subunit (red line) and  $0.5 \mu\text{g}$  of the Stx2a B subunit (blue line) were overlaid on the same plot. One of three representative experiments is shown for the aggregate data.

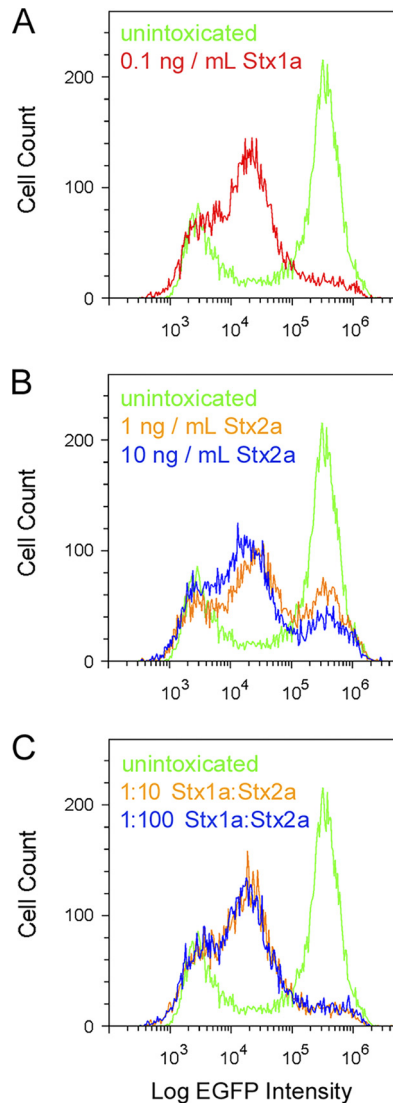


**FIG 5** Competition between Stx1a and Stx2a. Vero-d2EGFP cells were processed for cytofluorometry after an 18-h incubation with Stx1a (A), Stx2a (B), or a mixture of both toxins (C). In panel C, the orange trace represents cells incubated with a mixture of 0.1 ng/ml Stx1a and 1 ng/ml Stx2a, whereas the blue trace represents cells incubated with a mixture of 0.1 ng/ml Stx1a and 10 ng/ml Stx2a. Unintoxicated Vero-d2EGFP cells were also processed for each condition.

inhibition of protein synthesis. Cells exposed to toxin mixtures consisting of a 10-fold (orange) or 100-fold (blue) molar excess of Stx2a over Stx1a exhibited a uniform drop of protein synthesis that was similar to the fluorescent profile of cells exposed to Stx1a alone (Fig. 5C). Thus, Stx2a does not appear to effectively compete with Stx1a for binding to functional receptors on the target cell. A recent study documented the reduced potency of Stx2a in cell culture and animal models when mixed with the Stx1a B subunit (48), but our current work—which was only possible because of the different population responses to Stx1a versus Stx2a—provides the first experimental evidence that the Stx1a holotoxin can outcompete Stx2a in a cell culture model of intoxication.

**The identity of the B pentamer is responsible, in part, for the bimodal response observed with Stx2 subtypes.** Our collective results suggested that the different cellular responses to Stx1a versus Stx2a resulted from more Stx1a binding to the target cell. In this model, the origin of the toxin B subunit may determine whether the response to intoxication is uniform or bimodal. To test this model, we used two hybrid toxins that consisted of either the A1 subunit from Stx2a with the A2 and B subunits

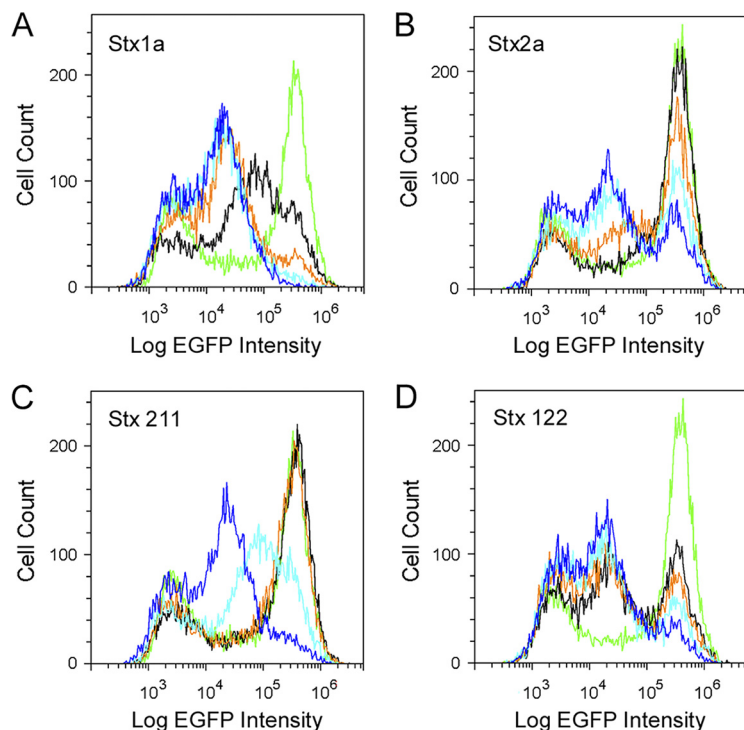


**FIG 6** Cellular response to hybrid toxins. Vero-d2EGFP cells were processed for cytofluorometry after an 18-h incubation with 10-fold serial dilutions of cell extracts from a nonpathogenic (Stx<sup>-</sup>) BL21 *E. coli* strain that was transformed with expression vectors encoding wild-type Stx1a (A), wild-type Stx2a (B), the 211 hybrid toxin consisting of the A1 subunit from Stx2a with the A2 and B subunits from Stx1a (C), or the 122 hybrid toxin consisting of the A1 subunit from Stx1a with the A2 and B subunits from Stx2a (D). The dilutions represented by each colored trace are as follows: black, 1:100,000; orange, 1:10,000; light blue, 1:1,000; blue, 1:100. Untreated Vero-d2EGFP cells are represented by the green trace.

from Stx1a (Stx 211) or the A1 subunit from Stx1a with the A2 and B subunits from Stx2a (Stx 122). The A2 linker is matched to its cognate B subunit in these chimeric toxins because it is important for holotoxin stability (38, 49, 50). Russo et al. (38) have shown that, in cultured cells and mice, the Stx 211 hybrid is more toxic than wild-type Stx2a, while the Stx 122 hybrid is less toxic than wild-type Stx1a. For the current study, we isolated both hybrid toxins from cell extracts of transformed *E. coli* strain BL21(DE3)pLysS. A control experiment demonstrated that the cell extract from untransformed *E. coli* did not have an effect on protein synthesis when added to the culture medium of Vero-d2EGFP cells (data not shown). Additional control experiments ensured that cell extracts containing wild-type Stx1a (Fig. 6A) or wild-type Stx2a (Fig. 6B) produced the expected responses that were previously observed using purified toxins (i.e., a uniform loss of protein synthesis in cells exposed to Stx1a and a bimodal response in cells exposed to Stx2a; Fig. 2 and 5). Vero-d2EGFP cells challenged with the Stx 211 hybrid toxin exhibited a uniform downward shift in protein synthesis (Fig. 6C) similar to that of wild-type Stx1a. In contrast, exposure to the Stx 122 hybrid toxin produced a bimodal response from the Vero-d2EGFP cells (Fig. 6D) that was similar to the response elicited by wild-type Stx2a. These results suggest that the A2 fragment and B subunit of a Stx contribute to the different population responses between Stx1a and Stx2a, as observed by flow cytometry, resulting in a uniform profile for toxins containing the B subunit of Stx1a and a bimodal profile for toxins containing the B subunit of Stx2a.

## DISCUSSION

Most quantitative assays that monitor the toxin-induced inhibition of protein synthesis and resulting cell death average the results from a population of cells (51, 52). Using these methods, it is not possible to differentiate between intoxicated and



unintoxicated cells within the population. As an alternative approach, we used flow cytometry in conjunction with a Vero-d2EGFP cell line that expresses an EGFP variant with a 2-h half-life. This allowed us to record the toxin-induced inhibition of protein synthesis and resulting loss of EGFP fluorescence from individual cells in the population of toxin-challenged cells. All Vero-d2EGFP cells exposed to Stx1a were affected by the toxin and thus, as previously reported (41), exhibited a uniform drop in protein synthesis that was detected by EGFP signal intensity. Even at the lowest concentration of Stx1a (0.001 ng/ml), a minor population-wide drop in fluorescent intensity was detected. In contrast, the bimodal fluorescent profile of Vero-d2EGFP cells exposed to moderate concentrations of Stx2a or Stx2c indicated that a subpopulation of the toxin-challenged cells was completely resistant to these toxins and therefore maintained their full level of protein synthesis. This bimodal response to Stx2a or Stx2c has not been previously reported.

The uniform response to Stx1a and bimodal response to Stx2a or Stx2c could not be attributed to the lack of Gb3 receptor in a subpopulation of cells. The number of cells resistant to Stx2a or Stx2c decreased with increasing toxin concentration, which further indicated there is no subpopulation of Vero-d2EGFP cells with intrinsic resistance to Stx2 subtypes. However, Vero cells did exhibit more efficient binding to the B subunit of Stx1a than to that of Stx2a. Stx1a could also outcompete Stx2a, as cells challenged with a combination of Stx1a and Stx2a exhibited a population-wide loss of protein synthesis even when there was a 100-fold molar excess of Stx2a over Stx1a. Additional studies with hybrid toxins indicated that the uniform versus bimodal response to intoxication is linked to the subtype of the B subunit, with the B subunit from Stx2a producing a bimodal response. Our collective results thus suggest that the bimodal response to Stx2a or Stx2c involves relatively weak binding between Stx2 subtypes and the host cell that reduces the total cytosolic pool of toxin. In contrast, the relatively strong binding of Stx1a to its target cell ensured that all cells in the population received an effective dose of cytosolic toxin.

Stx1a exhibits a higher *in vitro* affinity for Gb3 than that seen for Stx2a (28, 33, 35–37). Our cell binding studies with fluorescent B subunits were consistent with those reports, although it should be noted that our studies were conducted with monomeric B subunits that bind with lower affinity than that of holotoxins or B pentamers. Our studies further suggested that all cells in the population could bind Stx2a. Resistance to Stx2a in a subpopulation of cells was therefore unlikely to result from a lack of toxin binding. The bimodal response to Stx2a may instead be linked to the preferential binding of Stx2a to Gb3 isoforms that are not transported from the cell surface to the ER. Tam et al. (53) documented efficient binding of Stx1a but not Stx2a to Gb3 associated with the detergent-resistant membranes that undergo retrograde transport to the ER. Most cell-associated Stx2a binds nonproductively to a pool of Gb3 that does not traffic to the ER. This results in more efficient delivery of Stx1a than Stx2a to the ER and cytosol. Furthermore, Stx2a cannot compete with Stx1a for binding to Gb3 in detergent-resistant membranes (53). This observation is consistent with our intoxication assay, which demonstrated that a 100-fold molar excess of Stx2a cannot outcompete Stx1a, and with published work demonstrating that the B subunit from Stx1a reduces the toxicity of Stx2a (48). The bimodal response to Stx2 subtypes thus appears to result from two linked events that limit the cytosolic pool of Stx2 in comparison to Stx1a, namely, (i) relatively weak overall binding to the target cell, and (ii) a weaker interaction than Stx1a with the detergent-resistant membranes that are required for toxin transport to the ER and cytosol.

As we have previously demonstrated with Stx1a (41), cell death is not an inevitable outcome of toxin binding or even of toxin activity in the cytosol. We recently provided compelling evidence for this conclusion by demonstrating cells can recover from exposure to low toxin concentrations that, as detected with our Vero-d2EGFP assay, produced an initial population-wide reduction in protein synthesis (41). Removal of Stx1a from the medium was sufficient for cellular recovery (41). Here, the upward trend in cell viability after continual 72-h intoxication further suggested that it is possible for

cells to survive an ongoing toxin challenge and continue to grow. It remains to be determined whether these metabolically active cells recovered from intoxication or were never affected by the toxin. It should be noted, however, that Lentz et al. (54) reported a 100% loss of Vero cell viability after a continual 72-h exposure to the same concentrations of Stx1a and Stx2a used in the experiments shown in Fig. 1. Differences in relative potency of the applied toxins, protocol details, or other factors could account for this discrepancy. Additional work will be required to resolve this issue and to determine how the cellular outcome of intoxication is affected by the method of toxin application (i.e., pulsed exposure versus continual incubation).

Our collective work suggests therapeutic approaches that involve toxin neutralization at a postexposure stage could be effective strategies for the treatment of STEC infections and other toxin-mediated diseases. Experimental support for this concept has been generated in cell culture using neutralizing antibodies against Stx2a or the plant toxin ricin (55–57). These strategies may be particularly effective against STEC strains that express a Stx2 subtype, as the dose-dependent bimodal response to Stx2a or Stx2c suggests that it is possible to reduce the cell-associated pool of toxin to the point where cells are either completely resistant to intoxication or more prone to recover from a partial inhibition of protein synthesis. There also appears to be a natural decline in the levels of circulating Stx2a during human STEC infections (58), which could improve the possible success of treatments based on toxin neutralization after the onset of symptoms. Toxin inactivation could involve the administration of inactive Stx1a variants that compete with Stx2a for binding to target cells. This approach has been shown to reduce the toxicity of Stx2a in mice (48, 59). Neutralizing antibodies could likewise reduce the amount of Stx2a that reaches the cytosol of host cells, either by blocking adherence to the target cell or by disrupting intracellular toxin trafficking (60, 61).

Our data showing that Stx1a is more potent against cultured cells than Stx2 subtypes were consistent with published work (28, 29, 62). Our observation that Stx2a binds to target cells with lower affinity than that of Stx1a is also consistent with the literature (28, 33, 35, 37). However, those previous studies averaged the results from an entire population of toxin-challenged cells and could not detect variable responses within the subpopulations of cells. The use of a cytofluorometry-based intoxication assay allowed us, for the first time, to document the bimodal population response to Stx2 subtypes that appears to result from relatively poor toxin binding to Gb3 isoforms present in detergent-resistant membranes on the cell surface. These findings provide a new basis to better understand the differential toxicity between Stx subtypes and establish a conceptual foundation for the development of postexposure toxin therapeutics that function by lowering the amount of toxin that reaches the host cytosol.

## MATERIALS AND METHODS

**Materials.** Purified Stx1a (catalog no. NR-857, batches 60861998 and 70004145), Stx2a (catalog no. NR-4478, batches 58044918 and 63732536), and Stx2c (catalog no. NR-13422, batch 58582673) were obtained from BEI Resources (Manassas, VA). The monomeric B subunits from Stx1a (catalog no. NR-860, batch 59926594) and Stx2a (catalog no. NR-4677, batch 59019949, and catalog no. NR-49262, batch 63709686), also from BEI Resources, were conjugated to Alexa Fluor 594 using the Molecular Probes Alexa Fluor 594 microscale protein labeling kit (catalog no. A30008; Thermo Fisher Scientific, Waltham, MA). Plasmids encoding wild-type and hybrid Stxs (pLPSH3, pJES120, pMJS122, and pMJS211) were kindly provided by Angela Melton-Celsa (Department of Microbiology and Immunology, Uniformed Services University of the Health Sciences, Bethesda, MD). Toxin-containing cell extracts from transformed *E. coli* strain BL21 (DE3)pLysS were generated following a previously established protocol (63).

Generation of the Vero-d2EGFP cell line, which expresses a destabilized variant of the enhanced green fluorescent protein (d2EGFP), was previously described (64). Vero and Vero-d2EGFP cells were grown at 37°C under 5% CO<sub>2</sub> in Ham's F-12 medium (Life Technologies, Carlsbad, CA) containing 10% fetal bovine serum. Antibodies against Gb3/CD77 and Gb4 were purchased from GeneTex, Inc. (catalog no. GTX30743; Irvine, CA) and Matreya, LLC (catalog no. 1960; State College, PA), respectively. A goat anti-rat IgG antibody conjugated to allophycocyanin (APC) and a donkey anti-rabbit IgG antibody conjugated to phycoerythrin (PE) were purchased from Thermo Fisher Scientific (catalog no. A10540 and 12-4739-81, respectively).

**Toxicity assays.** Measurements of toxin activity by 3-(4,5-dimethylthiazol-2-yl)-5-(3-carboxymethoxyphenyl)-2-(4-sulfophenyl)-2H-tetrazolium (MTS) assay (Promega, Madison, WI), EGFP fluorescence with a

plate reader, or EGFP fluorescence with flow cytometry were performed as previously described (41, 65). In brief, a Synergy H1 multimode microplate reader (BioTek, Winooski, VT) was used for MTS measurements of 20,000 Vero-d2EGFP cells in a 96-well plate. MTS records metabolic activity, which is an indirect measure of cell viability. Background from the empty wells was subtracted from MTS experimental results. The background-subtracted values were then expressed as percentages of the control value recorded for unintoxicated cells. As a control to ensure substantial cell death could be detected, cells were incubated with 20% dimethyl sulfoxide (DMSO). The Synergy H1 multimode microplate reader with bottom optics position and 485-nm excitation/528-nm emission filter set was also used for EGFP fluorescence measurements with black-walled, clear-bottomed 96-well plates. Autofluorescence from the parental Vero cells that do not express EGFP was subtracted from experimental results with the Vero-d2EGFP cells. The background-subtracted values were then expressed as percentages of the control value recorded for unintoxicated Vero-d2EGFP cells. An Accuri C6 flow cytometer (BD Biosciences, San Jose, CA) or CytoFlex flow cytometer (Beckman Coulter Life Sciences, Indianapolis, IN) was used for cytofluorometry measurements of 10,000 cells per condition. As we previously reported (41, 65) and as can be seen here in the cytofluorometry data for unintoxicated cells, a minor population of Vero-d2EGFP cells do not express the EGFP construct despite ongoing selective pressure with G418. These nonexpressing cells served as an internal control in several experiments by marking the lower limit of fluorescent intensity that could be attained for the entire population of toxin-treated Vero-d2EGFP cells.

**Gb3 and Gb4 staining.** Vero cells seeded on a 10-cm dish 2 days before staining were allowed to reach about 90% confluence. They were then lifted from the dish with trypsin-EDTA and transferred to microcentrifuge tubes at a quantity of ~500,000 cells per tube. Cells were collected by centrifugation for 2 min at  $8,000 \times g$ , washed once with phosphate-buffered saline (PBS), and incubated under moderate shaking at 4°C for 2 h in Ham's F-12 medium containing 2% bovine serum albumin (BSA) and a 1:250 dilution of either a rat anti-Gb3 antibody or a rabbit anti-Gb4 antibody. The cells were then washed once with PBS and incubated under moderate shaking at 4°C for 1 h in Ham's F-12 medium containing 2% BSA and a 1:250 dilution of either an APC-conjugated goat anti-rat IgG antibody or a PE-conjugated donkey anti-rabbit IgG antibody. The cells were then washed with PBS, resuspended in 400  $\mu$ l of PBS, and processed using an Accuri C6 flow cytometer. When indicated, both anti-Gb3 and anti-Gb4 antibodies were added to the same population of Vero cells. To establish the background level of fluorescence, cells were exposed to the secondary antibodies alone.

**B subunit binding assay.** Vero or Vero-d2EGFP cells were handled as described above for Gb3 and Gb4 staining. Cells in suspension were incubated under moderate shaking at 4°C for 30 min in Ham's F-12 medium containing 2% BSA and various concentrations of the labeled B subunit from either Stx1a or Stx2a. The cells were then washed with PBS, resuspended in 400  $\mu$ l of PBS, and processed using an Accuri C6 flow cytometer. Cells incubated in the absence of toxin were used to establish the background level of autofluorescence. Pilot experiments found that cells exposed to an unlabeled toxin B subunit exhibited a fluorescent output similar to that of cells incubated without a toxin B subunit.

## ACKNOWLEDGMENTS

The following reagents were obtained through BEI Resources, NIAID, NIH: Shiga toxin type 1, recombinant from *Escherichia coli*, NR-857; Shiga toxin type 2, recombinant from *Escherichia coli*, NR-4478; Shiga toxin type 2 variant C (Stx2c), recombinant from *Escherichia coli*, NR-13422; Shiga toxin type 1 subunit B, recombinant from *Escherichia coli*, NR-860; Shiga toxin type 2 subunit B, recombinant from *Escherichia coli*, NR-4677 and NR-49262.

We thank Angela Melton-Celsa (Department of Microbiology and Immunology, Uniformed Services University of the Health Sciences, Bethesda, MD) for providing expression plasmids encoding wild-type or hybrid Stxs.

This material is based upon work supported by the U.S. Department of Agriculture (USDA), Agricultural Research Service, CRIS project 2030-42000-051-00D under Non-Assistance Cooperative Agreement (NACA) 58-5325-4-024. Any opinions, findings, conclusions, or recommendations expressed in this publication are those of the authors and do not necessarily reflect the view of the USDA.

## REFERENCES

- Melton-Celsa A, Mohawk K, Teel L, O'Brien A. 2012. Pathogenesis of Shiga-toxin producing *Escherichia coli*. *Curr Top Microbiol Immunol* 357:67–103. [https://doi.org/10.1007/82\\_2011\\_176](https://doi.org/10.1007/82_2011_176).
- Karmali MA. 2018. Factors in the emergence of serious human infections associated with highly pathogenic strains of shiga toxin-producing *Escherichia coli*. *Int J Med Microbiol* 308:1067–1072. <https://doi.org/10.1016/j.ijmm.2018.08.005>.
- Lee MS, Koo S, Jeong DG, Tesh VL. 2016. Shiga toxins as multi-functional proteins: induction of host cellular stress responses, role in pathogenesis and therapeutic applications. *Toxins* 8:77. <https://doi.org/10.3390/toxins8030077>.
- Besser RE, Griffin PM, Slutsker L. 1999. *Escherichia coli* O157:H7 gastroenteritis and the hemolytic uremic syndrome: an emerging infectious disease. *Annu Rev Med* 50:355–367. <https://doi.org/10.1146/annurev.med.50.1.355>.
- Tack DM, Marder EP, Griffin PM, Cieslak PR, Dunn J, Hurd S, Scallan E, Lathrop S, Muse A, Ryan P, Smith K, Tobin-D'Angelo M, Vugia DJ, Holt KG, Wolpert BJ, Tauxe R, Geissler AL. 2019. Preliminary incidence and trends

- of infections with pathogens transmitted commonly through food—foodborne diseases active surveillance network, 10 U.S. sites, 2015–2018. *MMWR Morb Mortal Wkly Rep* 68:369–373. <https://doi.org/10.15585/mmwr.mm6816a2>.
6. Pickering LK, Obrig TG, Stapleton FB. 1994. Hemolytic-uremic syndrome and enterohemorrhagic *Escherichia coli*. *Pediatr Infect Dis J* 13:459–475. <https://doi.org/10.1097/00006454-199406000-00001>.
  7. Olsnes S, Reisbig R, Eiklid K. 1981. Subunit structure of *Shigella* cytotoxin. *J Biol Chem* 256:8732–8738.
  8. Khine AA, Lingwood CA. 1994. Capping and receptor-mediated endocytosis of cell-bound verotoxin (Shiga-like toxin). 1: Chemical identification of an amino acid in the B subunit necessary for efficient receptor glycolipid binding and cellular internalization. *J Cell Physiol* 161: 319–332. <https://doi.org/10.1002/jcp.1041610217>.
  9. Lingwood CA. 1999. Glycolipid receptors for verotoxin and *Helicobacter pylori*: role in pathology. *Biochim Biophys Acta* 1455:375–386. [https://doi.org/10.1016/s0925-4439\(99\)00062-9](https://doi.org/10.1016/s0925-4439(99)00062-9).
  10. Sandvig K, van Deurs B. 1996. Endocytosis, intracellular transport, and cytotoxic action of Shiga toxin and ricin. *Physiol Rev* 76:949–966. <https://doi.org/10.1152/physrev.1996.76.4.949>.
  11. Garred O, van Deurs B, Sandvig K. 1995. Furin-induced cleavage and activation of Shiga toxin. *J Biol Chem* 270:10817–10821. <https://doi.org/10.1074/jbc.270.18.10817>.
  12. Garred O, Dubinina E, Polesskaya A, Olsnes S, Kozlov J, Sandvig K. 1997. Role of the disulfide bond in Shiga toxin A-chain for toxin entry into cells. *J Biol Chem* 272:11414–11419. <https://doi.org/10.1074/jbc.272.17.11414>.
  13. Endo Y, Tsurugi K, Yutsudo T, Takeda Y, Ogasawara T, Igarashi K. 1988. Site of action of a Vero toxin (VT2) from *Escherichia coli* O157:H7 and of Shiga toxin on eukaryotic ribosomes: RNA *N*-glycosidase activity of the toxins. *Eur J Biochem* 171:45–50. <https://doi.org/10.1111/j.1432-1033.1988.tb13756.x>.
  14. Obrig TG, Moran TP, Brown JE. 1987. The mode of action of Shiga toxin on peptide elongation of eukaryotic protein synthesis. *Biochem J* 244: 287–294. <https://doi.org/10.1042/bj2440287>.
  15. Strockbine NA, Marques LR, Newland JW, Smith HW, Holmes RK, O'Brien AD. 1986. Two toxin-converting phages from *Escherichia coli* O157:H7 strain 933 encode antigenically distinct toxins with similar biologic activities. *Infect Immun* 53:135–140.
  16. Scheutz F, Teel LD, Beutin L, Pierard D, Buvens G, Karch H, Mellmann A, Caprioli A, Tozzoli R, Morabito S, Strockbine NA, Melton-Celsa AR, Sanchez M, Persson S, O'Brien AD. 2012. Multicenter evaluation of a sequence-based protocol for subtyping Shiga toxins and standardizing Stx nomenclature. *J Clin Microbiol* 50:2951–2963. <https://doi.org/10.1128/JCM.00860-12>.
  17. Zheng J, Cui S, Teel LD, Zhao S, Singh R, O'Brien AD, Meng J. 2008. Identification and characterization of Shiga toxin type 2 variants in *Escherichia coli* isolates from animals, food, and humans. *Appl Environ Microbiol* 74:5645–5652. <https://doi.org/10.1128/AEM.00503-08>.
  18. Schmidt H, Scheef J, Morabito S, Caprioli A, Wieler LH, Karch H. 2000. A new Shiga toxin 2 variant (Stx2f) from *Escherichia coli* isolated from pigeons. *Appl Environ Microbiol* 66:1205–1208. <https://doi.org/10.1128/aem.66.3.1205-1208.2000>.
  19. Ito H, Terai A, Kurazono H, Takeda Y, Nishibuchi M. 1990. Cloning and nucleotide sequencing of Vero toxin 2 variant genes from *Escherichia coli* O91:H21 isolated from a patient with the hemolytic uremic syndrome. *Microb Pathog* 8:47–60. [https://doi.org/10.1016/0882-4010\(90\)90007-D](https://doi.org/10.1016/0882-4010(90)90007-D).
  20. Johannes L, Romer W. 2010. Shiga toxins—from cell biology to biomedical applications. *Nat Rev Microbiol* 8:105–116. <https://doi.org/10.1038/nrmicro2279>.
  21. Boerlin P, McEwen SA, Boerlin-Petzold F, Wilson JB, Johnson RP, Gyles CL. 1999. Associations between virulence factors of Shiga toxin-producing *Escherichia coli* and disease in humans. *J Clin Microbiol* 37:497–503.
  22. Bielaszewska M, Friedrich AW, Aldick T, Schürk-Bulgrin R, Karch H. 2006. Shiga toxin activatable by intestinal mucus in *Escherichia coli* isolated from humans: predictor for a severe clinical outcome. *Clin Infect Dis* 43:1160–1167. <https://doi.org/10.1086/508195>.
  23. Delannoy S, Mariani-Kurkdjian P, Bonacorsi S, Liguori S, Fach P. 2015. Characteristics of emerging human-pathogenic *Escherichia coli* O26: H11 strains isolated in France between 2010 and 2013 and carrying the *stx2d* gene only. *J Clin Microbiol* 53:486–492. <https://doi.org/10.1128/JCM.02290-14>.
  24. Bunger J, Melton-Celsa A, Maynard E, O'Brien A. 2015. Reduced toxicity of Shiga toxin (Stx) type 2c in mice compared to Stx2d is associated with instability of Stx2c holotoxin. *Toxins* 7:2306–2320. <https://doi.org/10.3390/toxins7062306>.
  25. Kawano K, Okada M, Haga T, Maeda K, Goto Y. 2008. Relationship between pathogenicity for humans and stx genotype in Shiga toxin-producing *Escherichia coli* serotype O157. *Eur J Clin Microbiol Infect Dis* 27:227–232. <https://doi.org/10.1007/s10096-007-0420-3>.
  26. Nataro JP, Kaper JB. 1998. Diarrheagenic *Escherichia coli*. *Clin Microbiol Rev* 11:142–201. <https://doi.org/10.1128/CMR.11.1.142>.
  27. Legros N, Pohlentz G, Steil D, Müthing J. 2018. Shiga toxin-glycosphingolipid interaction: status quo of research with focus on primary human brain and kidney endothelial cells. *Int J Med Microbiol* 308:1073–1084. <https://doi.org/10.1016/j.ijmm.2018.09.003>.
  28. Tesh VL, Burris JA, Owens JW, Gordon VM, Wadolowski EA, O'Brien AD, Samuel JE. 1993. Comparison of the relative toxicities of Shiga-like toxins type I and type II for mice. *Infect Immun* 61:3392–3402.
  29. Fuller CA, Pellino CA, Flagler MJ, Strasser JE, Weiss AA. 2011. Shiga toxin subtypes display dramatic differences in potency. *Infect Immun* 79: 1329–1337. <https://doi.org/10.1128/IAI.01182-10>.
  30. Jackson MP, Newland JW, Holmes RK, O'Brien AD. 1987. Nucleotide sequence analysis of the structural genes for Shiga-like toxin I encoded by bacteriophage 933J from *Escherichia coli*. *Microb Pathog* 2:147–153. [https://doi.org/10.1016/0882-4010\(87\)90106-9](https://doi.org/10.1016/0882-4010(87)90106-9).
  31. Tesh VL, O'Brien AD. 1991. The pathogenic mechanisms of Shiga toxin and the Shiga-like toxins. *Mol Microbiol* 5:1817–1822. <https://doi.org/10.1111/j.1365-2958.1991.tb00805.x>.
  32. Flagler MJ, Mahajan SS, Kulkarni AA, Iyer SS, Weiss AA. 2010. Comparison of binding platforms yields insights into receptor binding differences between Shiga toxins 1 and 2. *Biochemistry* 49:1649–1657. <https://doi.org/10.1021/bi902084y>.
  33. Head SC, Karmali MA, Lingwood CA. 1991. Preparation of VT1 and VT2 hybrid toxins from their purified dissociated subunits. Evidence for B subunit modulation of a subunit function. *J Biol Chem* 266:3617–3621.
  34. Lindgren SW, Samuel JE, Schmitt CK, O'Brien AD. 1994. The specific activities of Shiga-like toxin type II (SLT-II) and SLT-II-related toxins of enterohemorrhagic *Escherichia coli* differ when measured by Vero cell cytotoxicity but not by mouse lethality. *Infect Immun* 62:623–631.
  35. Lingwood CA. 1996. Role of verotoxin receptors in pathogenesis. *Trends Microbiol* 4:147–153. [https://doi.org/10.1016/0966-842X\(96\)10017-2](https://doi.org/10.1016/0966-842X(96)10017-2).
  36. Zumbun SD, Hanson L, Sinclair JF, Freedy J, Melton-Celsa AR, Rodriguez-Canales J, Hanson JC, O'Brien AD. 2010. Human intestinal tissue and cultured colonic cells contain globotriaosylceramide synthase mRNA and the alternate Shiga toxin receptor globotetraosylceramide. *Infect Immun* 78:4488–4499. <https://doi.org/10.1128/IAI.00620-10>.
  37. Karve SS, Weiss AA. 2014. Glycolipid binding preferences of Shiga toxin variants. *PLoS One* 9:e101173. <https://doi.org/10.1371/journal.pone.0101173>.
  38. Russo LM, Melton-Celsa AR, Smith MJ, O'Brien AD. 2014. Comparisons of native Shiga toxins (Stxs) type 1 and 2 with chimeric toxins indicate that the source of the binding subunit dictates degree of toxicity. *PLoS One* 9:e93463. <https://doi.org/10.1371/journal.pone.0093463>.
  39. Basu D, Li XP, Kahn JN, May KL, Kahn PC, Tumer NE. 2016. The A1 subunit of Shiga toxin 2 has higher affinity for ribosomes and higher catalytic activity than the A1 subunit of Shiga toxin 1. *Infect Immun* 84:149–161. <https://doi.org/10.1128/IAI.00994-15>.
  40. Quinones B, Massey S, Friedman M, Swimley MS, Teter K. 2009. Novel cell-based method to detect Shiga toxin 2 from *Escherichia coli* O157:H7 and inhibitors of toxin activity. *Appl Environ Microbiol* 75:1410–1416. <https://doi.org/10.1128/AEM.02230-08>.
  41. Cherubin P, Quinones B, Teter K. 2018. Cellular recovery from exposure to sub-optimal concentrations of AB toxins that inhibit protein synthesis. *Sci Rep* 8:2494. <https://doi.org/10.1038/s41598-018-20861-9>.
  42. Waddell T, Head S, Petric M, Cohen A, Lingwood C. 1988. Globotriaosylceramide is specifically recognized by the *Escherichia coli* verocytotoxin 2. *Biochem Biophys Res Commun* 152:674–679. [https://doi.org/10.1016/s0006-291x\(88\)80091-3](https://doi.org/10.1016/s0006-291x(88)80091-3).
  43. DeGrandis S, Law H, Brunton J, Gyles C, Lingwood CA. 1989. Globotetraosylceramide is recognized by the pig edema disease toxin. *J Biol Chem* 264:12520–12525.
  44. Samuel JE, Perera LP, Ward S, O'Brien AD, Ginsburg V, Krivan HC. 1990. Comparison of the glycolipid receptor specificities of Shiga-like toxin type II and Shiga-like toxin type II variants. *Infect Immun* 58:611–618.
  45. Keusch GT, Jacewicz M, Acheson DW, Donohue-Rolfe A, Kane AV, Mc-

- Cluer RH. 1995. Globotriaosylceramide, Gb3, is an alternative functional receptor for Shiga-like toxin 2e. *Infect Immun* 63:1138–1141.
46. Tyrrell GJ, Ramotar K, Toye B, Boyd B, Lingwood CA, Brunton JL. 1992. Alteration of the carbohydrate binding specificity of verotoxins from Gal alpha 1-4Gal to GalNAc beta 1-3Gal alpha 1-4Gal and vice versa by site-directed mutagenesis of the binding subunit. *Proc Natl Acad Sci U S A* 89:524–528. <https://doi.org/10.1073/pnas.89.2.524>.
47. Boyd B, Lingwood C. 1989. Verotoxin receptor glycolipid in human renal tissue. *Nephron* 51:207–210. <https://doi.org/10.1159/000185286>.
48. Petro CD, Trojnar E, Sinclair J, Liu ZM, Smith M, O'Brien AD, Melton-Celsa A. 2019. Shiga toxin type 1a (Stx1a) reduces the toxicity of the more potent Stx2a *in vivo* and *in vitro*. *Infect Immun* 87:e00787-18. <https://doi.org/10.1128/IAI.00787-18>.
49. Fraser ME, Chernaia MM, Kozlov YV, James MN. 1994. Crystal structure of the holotoxin from *Shigella dysenteriae* at 2.5 Å resolution. *Nat Struct Biol* 1:59–64. <https://doi.org/10.1038/nsb0194-59>.
50. Fraser ME, Fujinaga M, Cherney MM, Melton-Celsa AR, Twiddy EM, O'Brien AD, James MNG. 2004. Structure of shiga toxin type 2 (Stx2) from *Escherichia coli* O157:H7. *J Biol Chem* 279:27511–27517. <https://doi.org/10.1074/jbc.M401939200>.
51. Bozza WP, Tolleson WH, Rivera Rosado LA, Zhang B. 2015. Ricin detection: tracking active toxin. *Biotechnol Adv* 33:117–123. <https://doi.org/10.1016/j.biotechadv.2014.11.012>.
52. Zhou Y, Li XP, Kahn JN, Tumer NE. 2018. Functional assays for measuring the catalytic activity of ribosome inactivating proteins. *Toxins (Basel)* 10:240. <https://doi.org/10.3390/toxins10060240>.
53. Tam P, Mahfoud R, Nutikka A, Khine AA, Binnington B, Paroutis P, Lingwood C. 2008. Differential intracellular transport and binding of verotoxin 1 and verotoxin 2 to globotriaosylceramide-containing lipid assemblies. *J Cell Physiol* 216:750–763. <https://doi.org/10.1002/jcp.21456>.
54. Lentz EK, Leyva-Illades D, Lee MS, Cherala RP, Tesh VL. 2011. Differential response of the human renal proximal tubular epithelial cell line HK-2 to Shiga toxin types 1 and 2. *Infect Immun* 79:3527–3540. <https://doi.org/10.1128/IAI.05139-11>.
55. Yermakova A, Klokk TI, Cole R, Sandvig K, Mantis NJ. 2014. Antibody-mediated inhibition of ricin toxin retrograde transport. *mBio* 5:e00995-13. <https://doi.org/10.1128/mBio.00995-13>.
56. Song K, Mize RR, Marrero L, Corti M, Kirk JM, Pincus SH. 2013. Antibody to ricin A chain hinders intracellular routing of toxin and protects cells even after toxin has been internalized. *PLoS One* 8:e62417. <https://doi.org/10.1371/journal.pone.0062417>.
57. Krautz-Peterson G, Chapman-Bonofiglio S, Boisvert K, Feng H, Herman IM, Tzipori S, Sheoran AS. 2008. Intracellular neutralization of Shiga toxin 2 by an A subunit-specific human monoclonal antibody. *Infect Immun* 76:1931–1939. <https://doi.org/10.1128/IAI.01282-07>.
58. Lopez EL, Contrini MM, Glatstein E, Ayala SG, Santoro R, Ezcurra G, Teplitz E, Matsumoto Y, Sato H, Sakai K, Katsuura Y, Hoshida S, Morita T, Harning R, Brookman S. 2012. An epidemiologic surveillance of Shiga-like toxin-producing *Escherichia coli* infection in Argentinean children: risk factors and serum Shiga-like toxin 2 values. *Pediatr Infect Dis J* 31:20–24. <https://doi.org/10.1097/INF.0b013e31822ea6cf>.
59. Russo LM, Melton-Celsa AR, O'Brien AD. 2016. Shiga toxin (Stx) type 1a reduces the oral toxicity of Stx type 2a. *J Infect Dis* 213:1271–1279. <https://doi.org/10.1093/infdis/jiv557>.
60. Melton-Celsa AR, O'Brien AD. 2014. New therapeutic developments against Shiga toxin-producing *Escherichia coli*. *Microbiol Spectr* 2:EHEC-0013-2013. <https://doi.org/10.1128/microbiolspec.EHEC-0013-2013>.
61. Tzipori S, Sheoran A, Akiyoshi D, Donohue-Rolfe A, Trachtman H. 2004. Antibody therapy in the management of Shiga toxin-induced hemolytic uremic syndrome. *Clin Microbiol Rev* 17:926–941. <https://doi.org/10.1128/CMR.17.4.926-941.2004>.
62. Bauwens A, Bielaszewska M, Kemper B, Langehanenberg P, von Bally G, Reichelt R, Mulac D, Humpf H-U, Friedrich AW, Kim KS, Karch H, Muthing J. 2011. Differential cytotoxic actions of Shiga toxin 1 and Shiga toxin 2 on microvascular and macrovascular endothelial cells. *Thromb Haemost* 105:515–528. <https://doi.org/10.1160/TH10-02-0140>.
63. Russo LM, Melton-Celsa AR, Smith MA, Smith MJ, O'Brien AD. 2014. Oral intoxication of mice with Shiga toxin type 2a (Stx2a) and protection by anti-Stx2a monoclonal antibody 11E10. *Infect Immun* 82:1213–1221. <https://doi.org/10.1128/IAI.01264-13>.
64. Massey S, Quinones B, Teter K. 2011. A cell-based fluorescent assay to detect the activity of Shiga toxin and other toxins that inhibit protein synthesis. *Methods Mol Biol* 739:49–59. [https://doi.org/10.1007/978-1-61779-102-4\\_5](https://doi.org/10.1007/978-1-61779-102-4_5).
65. Cherubin P, Quinones B, Elkahoui S, Yokoyama W, Teter K. 2017. A cell-based fluorescent assay to detect the activity of AB toxins that inhibit protein synthesis. *Methods Mol Biol* 1600:25–36. [https://doi.org/10.1007/978-1-4939-6958-6\\_3](https://doi.org/10.1007/978-1-4939-6958-6_3).